

# High-Purity Triggered Single-Photon Emission from Symmetric Single InAs/InP Quantum Dots around the Telecom C-Band Window

Anna Musiał,\* Paweł Holewa, Paweł Wyborski, Marcin Syperek, Andrei Kors, Johann Peter Reithmaier, Grzegorz Sęk, and Mohamed Benyoucef\*

The authors demonstrate pure triggered single-photon emission from quantum dots (QDs) around the telecommunication C-band window, with characteristics preserved under non-resonant excitation at saturation, that is, the highest possible, lifetime-limited emission rates. The direct measurement of emission dynamics reveals photoluminescence decay times in the range of (1.7–1.8) ns corresponding to maximal photon generation rates exceeding 0.5 GHz. The measurements of the second-order correlation function exhibit, for the best case, a lack of coincidences at zero time delay—no multiple photon events are registered within the experimental accuracy. This is achieved by exploiting a new class of low-density and in-plane symmetric InAs/InP QDs grown by molecular beam epitaxy on a distributed Bragg reflector, perfectly suitable for non-classical light generation for quantum optics experiments and quantum-secured fiber-based optical communication schemes.

The emission of high-purity single photons at the telecom spectral range around 1.55  $\mu\text{m}$  (telecom C-band window) is essential for long-haul quantum-secured communication due to compatibility with existing silica fiber networks.<sup>[1,2]</sup> Different approaches

to realize single photon sources (SPS) have been employed so far in this spectral range, including spontaneous parametric down conversion (SPDC),<sup>[3–5]</sup> defects in carbon nanotubes,<sup>[6]</sup> or epitaxial semiconductor quantum dots<sup>[7]</sup> (QDs). However, the SPDC is relying on a probabilistic photon emission process determined by conversion efficiency and impeding high generation rates making it unfavorable for efficient on-demand single photon generation. On the other hand, it is technologically challenging within a current technology to form an active part of a device out of carbon nanotubes making such approaches purely scientific or very futuristic. Therefore, the epitaxial QDs<sup>[7]</sup> emitting in the 3rd telecom spectral range seem to be the most promising quantum emitters constituting the mainly application-relevant

solution, although still facing a couple of challenges. QDs have already been proven to be suitable candidates for deterministic and practical high-quality SPS<sup>[8,9]</sup> as they are a good approximation of a two-level system which inherently emits single photons, however by now mostly demonstrated in the visible and near infrared range below 1  $\mu\text{m}$ .<sup>[2,10–12]</sup> In this spectral range, QDs are the sources providing the purest single photons with the second-order correlation function at zero time delay  $g^{(2)}(0)$  value of  $(7.5 \pm 1.6) \times 10^{-5}$ <sup>[13]</sup> and the highest emission rates.<sup>[14]</sup> Regarding single-photon purity, only single ions could be competing candidates,<sup>[15]</sup> but these are much less practical in terms of integration and scalability.

In the telecom range, two material systems are exploited: InAs/GaAs and InAs/InP. Although the InAs/GaAs nanostructures benefit from the well-established technology, achieving emission in the telecom C-band window within this system is not straightforward, and a challenging strain engineering is indispensable.<sup>[16]</sup> In this approach, the growth procedure is demanding and causes severe technological complications deteriorating the optical quality of the material.<sup>[17]</sup> Despite that, a single photon emission in the telecom C-band range from InAs QDs on InGaAs metamorphic buffer layers on a GaAs substrate has been recently presented<sup>[18]</sup> showing high fidelity of entanglement,<sup>[19]</sup> precise wavelength tunability,<sup>[20]</sup> and coherent control of a QD state combined with single-photon indistinguishability.<sup>[21]</sup> Although these dots are under impressive development,<sup>[22]</sup> they

Dr. A. Musiał, P. Holewa, P. Wyborski, Dr. M. Syperek, Prof. G. Sęk  
Laboratory for Optical Spectroscopy of Nanostructures  
Department of Experimental Physics, Faculty of Fundamental Problems  
of Technology  
Wrocław University of Science and Technology  
Wybrzeże Wyspiańskiego 27, 50–370 Wrocław, Poland  
E-mail: anna.musial@pwr.edu.pl

A. Kors, Prof. J. P. Reithmaier, Dr. M. Benyoucef  
Institute of Nanostructure Technologies and Analytics (INA)  
Center for Interdisciplinary Nanostructure Science and Technology  
(CINSaT)  
University of Kassel  
Heinrich-Plett-Str. 40 34132 Kassel, Germany  
E-mail: m.benyoucef@physik.uni-kassel.de

The ORCID identification number(s) for the author(s) of this article can be found under <https://doi.org/10.1002/qute.201900082>

© 2019 The Authors. Published by WILEY-VCH Verlag GmbH & Co. KGaA, Weinheim. This is an open access article under the terms of the Creative Commons Attribution License, which permits use, distribution and reproduction in any medium, provided the original work is properly cited.

DOI: 10.1002/qute.201900082

still struggle with some inherent difficulties, including non-zero fine structure splitting being a prerequisite for high entanglement fidelity of photons originating from biexciton–exciton cascade relevant for quantum communication schemes<sup>[23,24]</sup> or only partial suppression of multiphoton emission events under non-resonant pulsed excitation.<sup>[22]</sup> Although selective excitation schemes, resonant<sup>[21]</sup> or quasi-resonant,<sup>[25]</sup> can help in accessing the target QD only and suppressing the dephasing processes, and therefore greatly reduce the background emission and enhance the purity and coherence properties of single photons, they remain more challenging to realize and require tunable laser sources. For applications, where the purity of single photons is crucial, but high coherence is not indispensable, for example, quantum key distribution protocols (BB84), the non-resonant excitation is much easier to realize and more flexible. The investigated InAs/InP QDs provide pure single photon emission already under non-resonant excitation which makes them very promising for further exploitation in quantum technologies.

This alternative InAs/InP material system is actually the technologically easiest choice because such dots emit naturally in the 1.55  $\mu\text{m}$  range and no special strain engineering has to be applied, which allows overcoming some of the mentioned fabrication drawbacks of the GaAs-based materials. In addition, several matrices/barriers lattice-matched to InP can be considered, which gives additional freedom in modifying the confinement and strain, and hence giving convenient tuning knobs to tailor all the essential single dot characteristic.<sup>[26–31]</sup> There exist approaches able to give a lower spatial density of InAs on InP dots.<sup>[32,33]</sup> For instance, combining the InP matrix with the double-cap technique in metalorganic chemical vapor deposition (MOCVD) showed high suppression of multiphoton events under non-resonant<sup>[34]</sup> and quasi-resonant<sup>[35,36]</sup> excitation. MOCVD-grown structures allowed also for realization of single-photon emission under electrical carrier injection.<sup>[37]</sup> However, all of them lead to strongly anisotropic structures with FSS well above 20  $\mu\text{eV}$ <sup>[28,36,38]</sup> therefore limiting their applicability. Recently, another technological approach for realization of InP-based QDs, namely the droplet epitaxy growth has been reported.<sup>[39]</sup> This enabled the realization of quantum teleportation with average fidelity of  $88.3 \pm 4\%$  due to long time scale and high degree of coherence of emitted photons.

In this work, we present recent progress in terms of single-photon generation in yet another technological approach, that is, the molecular beam epitaxy (MBE) growth of InAs Stranski–Krastanow QDs embedded directly in InP matrix for which in-plane symmetry was achieved due to major modifications in the MBE growth by introducing a ripening step.<sup>[28,30,31]</sup> Bottom distributed Bragg reflector (DBR) structure (important but technologically demanding step reported rarely for this material system so far<sup>[28,31,39]</sup> due to requirement for high refractive index contrast layers lattice-matched to InP substrate) is introduced below the QD layer and provided more than one order of magnitude enhancement of photon extraction efficiency<sup>[31]</sup> enabling experiments on the single-photon level. Application of the ripening method reduces the QD areal density enhances the QD symmetry and in result reduces the FSS to the record level of  $\approx 2 \mu\text{eV}$ ,<sup>[30,31]</sup> making them very promising in view of generation of entangled photon pairs. However, the ripening step is not enough to achieve in-plane symmetric QDs and the material preceding the growth

of QD layer seems to be crucial as symmetric structures were achieved for InAs QDs grown directly in InP matrix,<sup>[31]</sup> but on the contrary, lower symmetry nanostructures were formed in the case of quaternary barrier.<sup>[28,33]</sup> Due to different interface, the reactions during the ripening step are different and the presence of the phosphorus atoms seems crucial. One of the parameters directly affecting QD properties is As-P exchange process during the growth of QDs. This addresses at once most of the challenges remaining for quantum emitters in the telecom C-band window: low QD spatial density and in-plane symmetry as well as the photon extraction efficiency and material quality which has been confirmed by the linewidths of single emission lines well below 50  $\mu\text{eV}$ .<sup>[31]</sup> However, no single-photon emission properties for such symmetric InAs/InP QDs have been reported so far, and hence it is the focus of this work aiming to fill this gap.

Figure 1a presents low-temperature  $\mu\text{PL}$  spectrum centered around the telecom C-band wavelength obtained under cw non-resonant excitation. The natural nanostructures' inhomogeneities in, for example, size, strain, and chemical content allow spanning the emission from below 1480 to above 1580 nm at least, depending on the position on the wafer. Therefore, the detected lines can overlap with all the three subranges of the 3rd telecom window, that is, the S-band (1460–1530 nm), C-band (1530–1565 nm), and L-band (1565–1625 nm), which can be an advantage of the considered system for applications allowing multiple parallel transmissions. Figure 1b,c present exemplary spectra for two bright QDs emitting in different spectral ranges within the 3rd telecom window selected based on their emission intensity and spectral isolation: longer-wavelength line A (between C- and L-band), and shorter-wavelength line B (S-band). These are good candidates to study single-photon generation which is the focus of this work. The other emission lines visible in these two spectra might originate from radiative recombination of different excitonic configurations in the QD or from different QD located in the same square-shaped mesas of 1  $\mu\text{m}$  size, but the exact identification of various excitonic complexes is beyond the scope of presented work (in particular, neutral biexciton and exciton emission has already been investigated in ref. [28]).

Selected emission lines were first characterized by means of power-dependent and polarization-resolved  $\mu\text{PL}$ . Their relatively high PL intensity is a fingerprint of the combined effects of high internal quantum efficiency of the emitters as well as the mesa- and DBR-enhanced photon extraction efficiency,<sup>[28,31]</sup> which according to calculations could result in the extraction efficiency higher than 20% (NA = 0.4) for further optimized layer structure (in particular layer thicknesses), mesa geometry, and QD positioned in the center of the mesa.<sup>[40]</sup>

Single emission lines in investigated sample are significantly narrower than typically observed for epitaxial nanostructures in this material system, similar to lines A and B ( $\approx 43$  and  $\approx 38 \mu\text{eV}$ , respectively). From the comparison to the emission linewidth obtained for a planar structure (the resolution limited linewidth of less than 35  $\mu\text{eV}$ ),<sup>[31]</sup> one may conclude about negligible influence of the charge environmental conditions after fabrication of the mesas suggesting that investigated QDs are relatively far from mesa sidewalls. Moreover, the observed linewidths are comparable to the best observed for GaAs-based QDs emitting in the 3rd telecom window ( $\approx 59 \mu\text{eV}$ )<sup>[18]</sup> and are much lower than  $\approx 200 \mu\text{eV}$

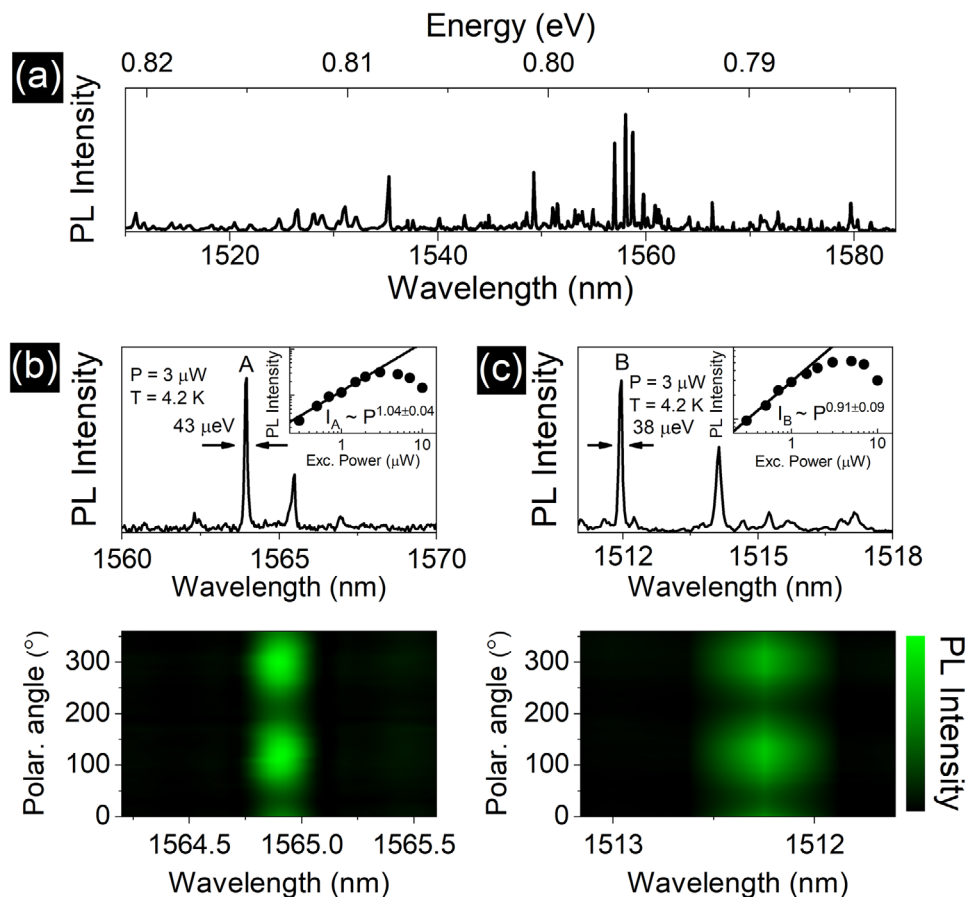


**Figure 1.**  $\mu$ PL spectra ( $T = 4.2$  K, cw non-resonant excitation) in a broad range (a) and in the narrow range for two exemplary QDs (top): b) long-wavelength, line A and c) short-wavelength, line B at excitation power corresponding to the saturation of emission. Insets in (b) and (c): dependence of PL intensity on excitation power fitted by the power function. Bottom: Polarization maps for line A and B.

observed for strongly elongated but naturally formed in MBE InAs/InP quantum dashes.<sup>[41]</sup>

Insets in Figure 1b,c with the excitation power dependent emission intensity of the selected lines show first the linear increase of PL intensity, and next the intensity saturation for excitation powers in the range of few microwatts, which is typical for emission from neutral or charged excitons (trions) confined in a QD. From the fact that both the lines are solely visible in the spectrum for the lowest excitation power, one can conclude that they most likely originate from recombination of carriers in their ground state. The polarization-resolved  $\mu$ PL shows that either line A or B cannot be characterized by a decisive linear polarization splitting within the spectral resolution of the experimental setup in agreement with previous statistical measurements showing small FSS below  $4 \mu\text{eV}$  and confirming in-plane symmetry of the QDs.<sup>[31]</sup> Therefore, other spectroscopic techniques would be required to distinguish between the charged and neutral excitonic complexes in this structure and to confirm unambiguously the origin of other emission lines visible in the spectrum, which was, however, unnecessary for the current study aiming at probing mainly the single photon emission characteristics.

The TRPL has been employed to investigate the carrier dynamics and identify the fundamental limit for the maximal repetition

rate in view of triggered SPS based on InAs/InP QDs under investigation. As previously stated, the existence of the lower DBR section in the sample gives high intensities of the observed emission lines. It allows for direct detection of time-resolved PL with a state-of-the-art NIR-enhanced streak camera having a time-resolution in the limit of 20 ps, comparable to typically used time-correlated single photon counting systems. The streak camera measurement allowed for obtaining spectro-temporal emission maps for the selected QDs presented in Figure 2. The PL traces for lines A and B are plotted on the right side of each map in the semi-logarithmic scale. The corresponding time-integrated PL spectra are additionally presented at the top of Figure 2. The spectra are consistent with those from Figure 1: the same emission lines are visible in the spectrum, and the relative intensities are similar. Also, the linewidth of the main spectral features is not altered. Regarding the PL decay time, it is similar for both lines within the experimental and fitting accuracy with  $\tau_A = (1.71 \pm 0.06)$  ns, and  $\tau_B = (1.79 \pm 0.03)$  ns for A, and B line, respectively, being rather typical for the InAs/InP nanostructures in general, independently of their exact size and symmetry.<sup>[29,35,41–45]</sup> These values correspond to generation rate of about 0.5 GHz, which is the fundamental upmost limit because it will further be reduced by the finite collection efficiency or other detection losses.

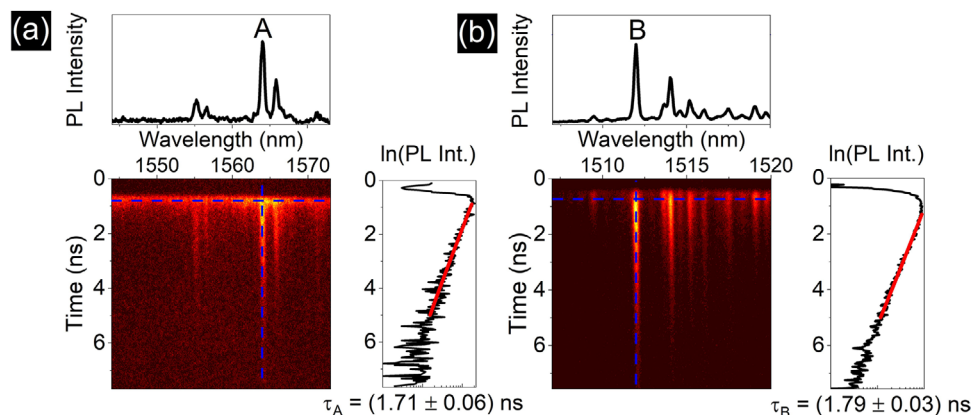


**Figure 2.** TRPL maps recorded on NIR-enhanced streak camera for a) line A and b) line B. Blue dashed lines indicate spectra (horizontal cross-section) and the PL time traces of A and B lines (vertical cross section). Top: PL spectra taken under non-resonant pulsed excitation. Right: PL decays fitted with monoexponential decay curves (red lines). Determined PL decay times are  $\tau_A = (1.71 \pm 0.06)$  ns and  $\tau_B = (1.79 \pm 0.03)$  ns.

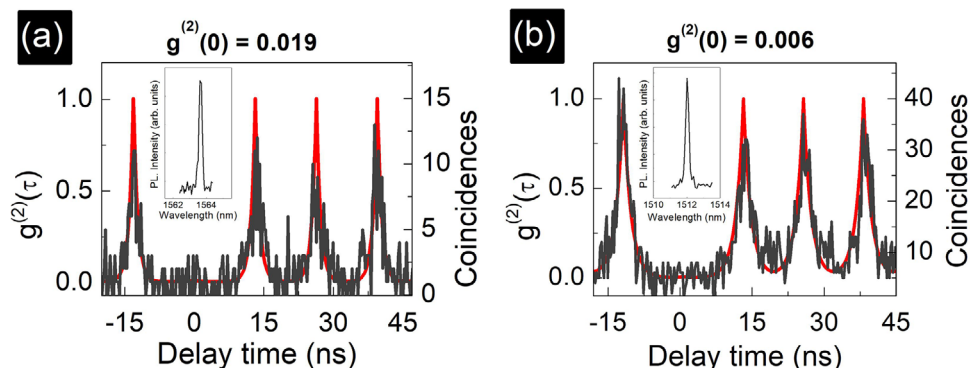


**Figure 3.** Autocorrelation histograms measured under pulsed excitation: a) quasi-resonant with  $\lambda_{\text{exc}} = 1460$  nm for line A and b) non-resonant for line B. Red lines fit to the experimental data with  $g^{(2)}(0)$  values of a) 0.019 and b) 0.006.

The main goal of the presented work is to verify the potential of the investigated InAs/InP QDs for realization of triggered SPS operating in the 3rd telecom window by evaluating probability of multiphoton events described by the second-order correlation function  $g^{(2)}(\tau)$ . It has been determined for the selected A and B emitters under quasi-resonant and non-resonant pulsed excitation, respectively, with the excitation power  $P_{\text{exc}}$  corresponding to the onset of lines' saturation (0.5 mW and 2  $\mu$ W, respectively) – **Figures 3a,b**. Quasi-resonant excitation has been chosen for line A due to lower signal to background ratio in comparison to line B deteriorating the single-photon purity. In **Figures 3a,b** anti-bunching behavior with very low number of photon coincidences at  $\tau = 0$  ns is clearly visible. The  $g^{(2)}(0)$  value determined for line B from the fit to experimental data<sup>[31]</sup> (solid red line) equals to  $g^{(2)}_{\text{fit}}(0) = 0.006$  with the standard error of Levenberg–Marquardt fitting procedure of 0.063, which proves that the investigated QD generates purely single triggered photons even under non-resonant excitation at the saturation power limit. In the case of the longer wavelength line A, the as-measured  $g^{(2)}(0) \approx 0$  translates into  $g^{(2)}_{\text{fit}}(0) = 0.019$  (standard error of 0.074) obtained from the fit proving triggered and pure single-photon emission with the emission wavelength around the telecom C-band. The abovementioned results evidence that both the investigated QD emitters are promising candidates for a triggered, telecom

single-photon source even at saturation power corresponding to the highest achievable emission rate.

In conclusion, we demonstrated triggered QD-based SPS of high single-photon emission purity operating at different wavelengths of the 3rd telecom window. It is achieved via ground-state exciton recombination from the new generation of MBE-grown in-plane symmetric InAs/InP QDs located on a distributed Bragg reflector. The obtained PL decay times are in the range of 1.7–1.8 ns, so that the corresponding maximal single-photon generation rate is estimated to be above 0.5 GHz. Such bright, true single-photon emitters pave the way toward practical implementations in quantum communication schemes in the long-haul fiber networks with the potential for high generation rates. Additionally, vanishing exciton fine structure splitting enables generation of entangled photon pairs from biexciton–exciton cascade, which is under investigation and will be reported elsewhere.

## Experimental Section

The structure under investigation was grown by MBE on a (100)-oriented InP substrate.<sup>[31]</sup> The QDs were formed by depositing nominally two monolayers of InAs on InP at a temperature  $T = 490$  °C combined with the ripening process resulting in low density of symmetric dots<sup>[31]</sup> (density from  $5 \times 10^8$  to  $2 \times 10^9$  cm<sup>-2</sup> in comparison to  $6 \times 10^9$  cm<sup>-2</sup>

achievable in GaAs-based structures<sup>[18]</sup> for the same spectral range). The QDs were placed on a DBR formed by 25 InP/InAlGaAs mirror pairs, for enhancement of the photon extraction efficiency, and were capped by a 100-nm-thick InP layer. The square-like mesa structures down to less than 1  $\mu\text{m}^2$  area have been processed on the sample surface using an e-beam lithography and wet chemical etching technique. They act as markers and facilitate long-term study of the same QD.

For all measurements, the sample was cooled down to  $T = 4.2$  K in a helium continuous-flow cryostat. QDs were excited non-resonantly either by a 660 nm line from a continuous-wave (cw) laser or an 80 MHz pulse train with  $\approx 50$  ps long pulses and an 805 nm wavelength from a semiconductor diode laser. For quasi-resonant pulsed excitation, an optical parametric oscillator generating 76 MHz train of pulses with  $\approx 2$  ps duration and pumped synchronously by the mode-locked Ti:Sapphire laser was used. QD emission was measured in a microphotoluminescence ( $\mu\text{PL}$ ) setup equipped with a 1 m focal length spectrometer based on a deeply cooled InGaAs linear detector, and a long working distance microscope objective (NA = 0.4) provided high spatial ( $\approx 1$   $\mu\text{m}$ ) and spectral ( $\approx 20$   $\mu\text{eV}$ ) resolution. For TRPL, single-dot emission was dispersed by a 0.3 m focal length monochromator and detected by an InGaAs-based near-infrared-enhanced streak camera sensitive up to 1600 nm. The overall time resolution of TRPL setup was  $\approx 20$  ps. Single-photon emission events from a QD were tested by the Hanbury-Brown and Twiss interferometer with a 0.32 m focal length monochromator acting as an  $\approx 0.4$  nm spectral band-pass filter enabling isolation of the target optical transition. The filtered signal was coupled into a single-mode fiber and detected by a pair of NbN superconducting single-photon counting modules with 15% quantum efficiency and 10 dark counts per second at 1.55  $\mu\text{m}$ . A multichannel picosecond event timer acquired the photon correlation statistics. The overall time resolution of the correlation setup was  $\approx 80$  ps.

## Acknowledgements

The authors acknowledge financial support via the “Quantum dot-based indistinguishable and entangled photon sources at telecom wavelengths” project, carried out within the HOMING programme of the Foundation for Polish Science co-financed by the EU under the EFRE. This work was also financially supported by the BMBF Project of German Federal Ministry of Education and Research (BMBF) (Q.Link.X), DFG (DeLiCom), and by the National Science Centre in Poland within grant No. 2014/14/M/ST3/00821.

## Conflict of Interest

The authors declare no conflict of interest.

## Keywords

molecular beam epitaxy, quantum dots, single-photon emission, spectroscopy, telecom-wavelength

Received: July 8, 2019

Revised: October 13, 2019

Published online: November 7, 2019

- [1] N. Gisin, R. Thew, *Nat. Photonics* **2007**, *1*, 165.
- [2] P. Senellart, G. Solomon, A. White, *Nat. Nanotechnol.* **2017**, *12*, 1026.
- [3] S. Fasel, O. Alibart, S. Tanzilli, P. Baldi, A. Beveratos, N. Gisin, H. Zbinden, *New J. Phys.* **2004**, *6*, 163.
- [4] Y. Yamamoto, C. Schneider, C. M. Natarajan, M. Kamp, S. Maier, V. Esfandyarpour, J. S. Pelc, S. Höfling, K. De Greve, R. H. Hadfield,

- M. M. Fejer, P. L. McMahon, L. Yu, A. Forchel, *Opt. Express* **2012**, *20*, 27510.
- [5] L. A. Ngah, O. Alibart, L. Labonté, V. D'Auria, S. Tanzilli, *Laser Photonics Rev.* **2015**, *9*, L1.
- [6] X. He, N. F. Hartmann, X. Ma, Y. Kim, R. Ihly, J. L. Blackburn, W. Gao, J. Kono, Y. Yomogida, A. Hirano, T. Tanaka, H. Kataura, H. Htoon, S. K. Doorn, *Nat. Photonics* **2017**, *11*, 577.
- [7] P. Michler, *Single Semiconductor Quantum Dots*, Springer-Verlag, Berlin **2009**.
- [8] M. Gschrey, A. Thoma, P. Schnauber, M. Seifried, R. Schmidt, B. Wohlfeil, L. Krüger, J.-H. Schulze, T. Heindel, S. Burger, F. Schmidt, A. Strittmatter, S. Rodt, S. Reitzenstein, *Nat. Commun.* **2015**, *6*, 7662.
- [9] X. Ding, Y. He, Z.-C. Duan, N. Gregersen, M.-C. Chen, S. Unsleber, S. Maier, C. Schneider, M. Kamp, S. Höfling, C.-Y. Lu, J.-W. Pan, *Phys. Rev. Lett.* **2016**, *116*, 020401.
- [10] S. Buckley, K. Rivoire, J. Vučković, *Rep. Prog. Phys.* **2012**, *75*, 126503.
- [11] Y. Yamamoto, C. Santori, G. Solomon, J. Vuckovic, D. Fattal, E. Waks, E. Diamanti, *Prog. Inf.* **2005**, *1*, 5.
- [12] W. W. Chow, S. Reitzenstein, *Appl. Phys. Rev.* **2018**, *5*, 041302.
- [13] L. Schweickert, K. D. Jöns, K. D. Zeuner, S. F. Covre da Silva, H. Huang, T. Lettner, M. Reindl, J. Zichi, R. Trotta, A. Rastelli, V. Zwiller, *Appl. Phys. Lett.* **2018**, *112*, 093106.
- [14] P. Lodahl, *Quantum Sci. Technol.* **2018**, *3*, 013001.
- [15] C. Crocker, M. Lichtman, K. Sosnova, A. Carter, S. Scarano, C. Monroe, *Opt. Express* **2019**, *27*, 28143.
- [16] E. S. Semenova, R. Hosten, G. Patriarcho, O. Mauguin, L. Largeau, I. Robert-Philip, A. Beveratos, A. Lemaître, *J. Appl. Phys.* **2008**, *103*, 103533.
- [17] L. Seravalli, G. Trevisi, P. Frigeri, D. Rivas, G. Muñoz-Matutano, I. Suárez, B. Alén, J. Canet-Ferrer, J. P. Martínez-Pastor, *Appl. Phys. Lett.* **2011**, *98*, 173112.
- [18] M. Paul, F. Olbrich, J. Höschele, S. Schreier, J. Kettler, S. L. Portalupi, M. Jetter, P. Michler, *Appl. Phys. Lett.* **2017**, *111*, 033102.
- [19] F. Olbrich, J. Höschele, M. Müller, J. Kettler, S. Luca Portalupi, M. Paul, M. Jetter, P. Michler, *Appl. Phys. Lett.* **2017**, *111*, 133106.
- [20] K. D. Zeuner, M. Paul, T. Lettner, C. Reuterskiöld Hedlund, L. Schweickert, S. Steinhauer, L. Yang, J. Zichi, M. Hammar, K. D. Jöns, V. Zwiller, *Appl. Phys. Lett.* **2018**, *112*, 173102.
- [21] C. Nawrath, F. Olbrich, M. Paul, S. L. Portalupi, M. Jetter, P. Michler, *Appl. Phys. Lett.* **2019**, *115*, 023103.
- [22] S. L. Portalupi, M. Jetter, P. Michler, *Semicond. Sci. Technol.* **2019**, *34*, 053001.
- [23] A. K. Ekert, *Phys. Rev. Lett.* **1991**, *67*, 661.
- [24] F. B. Basset, M. B. Rota, C. Schimpf, D. Tedeschi, K. D. Zeuner, S. F. C. da Silva, M. Reindl, V. Zwiller, K. D. Jöns, A. Rastelli, R. Trotta, arXiv:1901.06646v1 [quant-ph], **2019**.
- [25] K. Takemoto, S. Hirose, M. Takatsu, N. Yokoyama, Y. Sakuma, T. Usuki, T. Miyazawa, Y. Arakawa, *Phys. Status Solidi C* **2008**, *5*, 2699.
- [26] Ł. Dusanowski, M. Syperek, P. Mrowiński, W. Rudno-Rudziński, J. Misiewicz, A. Somers, S. Höfling, M. Kamp, J. P. Reithmaier, G. Şek, *Appl. Phys. Lett.* **2014**, *105*, 021909.
- [27] Ł. Dusanowski, M. Syperek, J. Misiewicz, A. Somers, S. Höfling, M. Kamp, J. P. Reithmaier, G. Şek, *Appl. Phys. Lett.* **2016**, *108*, 163108.
- [28] M. Benyoucef, M. Yacob, J. P. Reithmaier, J. Kettler, P. Michler, *Appl. Phys. Lett.* **2013**, *103*, 162101.
- [29] M. D. Birowosuto, H. Sumikura, S. Matsuo, H. Taniyama, P. J. Van Veldhoven, R. Nötzel, M. Notomi, *Sci. Rep.* **2012**, *2*, 321.
- [30] A. Kors, K. Fuchs, M. Yacob, J. P. Reithmaier, M. Benyoucef, *Appl. Phys. Lett.* **2017**, *110*, 031101.
- [31] A. Kors, J. P. Reithmaier, M. Benyoucef, *Appl. Phys. Lett.* **2018**, *112*, 172102.
- [32] K. Takemoto, Y. Sakuma, S. Hirose, T. Usuki, N. Yokoyama, *Jpn. J. Appl. Phys.* **2004**, *43*, L349.

- [33] M. Yacob, J. P. Reithmaier, M. Benyoucef, *Appl. Phys. Lett.* **2014**, *104*, 022113.
- [34] T. Miyazawa, K. Takemoto, Y. Sakuma, S. Hirose, T. Usuki, N. Yokoyama, M. Takatsu, Y. Arakawa, *Jpn. J. Appl. Phys.* **2005**, *44*, L620.
- [35] K. Takemoto, M. Takatsu, S. Hirose, N. Yokoyama, Y. Sakuma, T. Usuki, T. Miyazawa, Y. Arakawa, *J. Appl. Phys.* **2007**, *101*, 081720.
- [36] T. Miyazawa, K. Takemoto, Y. Nambu, S. Miki, T. Yamashita, H. Terai, M. Fujiwara, M. Sasaki, Y. Sakuma, M. Takatsu, T. Yamamoto, Y. Arakawa, *Appl. Phys. Lett.* **2016**, *109*, 132106.
- [37] T. Müller, J. Skiba-Szymanska, A. B. Krysa, J. Huwer, M. Felle, M. Anderson, R. M. Stevenson, J. Heffernan, D. A. Ritchie, A. J. Shields, *Nat. Commun.* **2018**, *9*, 862.
- [38] J. Skiba-Szymanska, R. M. Stevenson, C. Varnava, M. Felle, J. Huwer, T. Müller, A. J. Bennett, J. P. Lee, I. Farrer, A. B. Krysa, P. Spencer, L. E. Goff, D. A. Ritchie, J. Heffernan, A. J. Shields, *Phys. Rev. Appl.* **2017**, *8*, 014013.
- [39] M. Anderson, T. Müller, J. Huwer, J. Skiba-Szymanska, A. B. Krysa, R. M. Stevenson, J. Heffernan, D. A. Ritchie, A. J. Shields, arXiv:1901.02260, **2019**.
- [40] P. Mrowiński, G. Sęk, *Physica B* **2019**, *562*, 141.
- [41] Ł. Dusanowski, M. Gawelczyk, J. Misiewicz, S. Höfling, J.-P. Reithmaier, G. Sęk, *Appl. Phys. Lett.* **2018**, *113*, 043103.
- [42] Ł. Dusanowski, M. Syperek, W. Rudno-Rudziński, P. Mrowiński, G. Sęk, J. Misiewicz, A. Somers, J. P. Reithmaier, S. Höfling, A. Forchel, *Appl. Phys. Lett.* **2013**, *103*, 253113.
- [43] M. Syperek, Ł. Dusanowski, J. Andrzejewski, W. Rudno-Rudziński, G. Sęk, J. Misiewicz, F. Lelarge, *Appl. Phys. Lett.* **2013**, *103*, 083104.
- [44] T. Miyazawa, T. Nakaoka, T. Usuki, Y. Arakawa, K. Takemoto, S. Hirose, S. Okumura, M. Takatsu, N. Yokoyama, *Appl. Phys. Lett.* **2008**, *92*, 161104.
- [45] N. Chauvin, P. Nedel, C. Seassal, B. Ben Bakir, X. Letartre, M. Gendry, A. Fiore, P. Viktorovitch, *Phys. Rev. B* **2009**, *80*, 045315.